

Flux Growth of ^{57}Fe -enriched Very High Quality Iron Borate Single Crystal and Observation of Magnetic Domain Structure using X-ray Double Crystal Topography

Takaya Mitsui, Humihiko Takei¹, Shinji Kitao², Makoto Seto², Taikan Harami, Xiaowei Zhang³, Yoshitaka Yoda⁴, Seishi Kikuta⁴

Japan Atomic Energy Research Institute., Kamigori, Ako-gun, Hyogo 678-12, Japan

Fax: 0791-58-2740, e-mail: taka@spring8.or.jp

¹ Crystal Systems Inc., 9633 Kobuchizawa, Yamanashi 408-0044, Japan

Fax: 0551-36-5273, e-mail: h.takei@f2.dion.ne.jp

² Research Reactor Institute, Kyoto University., Kumatori, Sennan-gun, Osaka 590-0494, Japan

Fax: 0724-51-2631, e-mail: seto@rri.kyoto-u.ac.jp, kitao@rri.kyoto-u.ac.jp

³ High Energy Accelerator Research Organization., KEK, 1-1 Oho, Tsukuba, Ibaraki 305-0801 Japan

Fax: 0298-64-5796, e-mail: xiaowei@post.kek.jp

⁴ Japan Synchrotron Radiation Research Institute., 1-1-1 Kouto Mikazuki-cho Sayo-gun Hyogo 679-5198 Japan

Fax: 0791-58-0830, e-mail: yoda@spring8.or.jp

A high quality iron borate, $^{57}\text{FeBO}_3$, single crystal for Mössbauer single-line filtering optical element of synchrotron radiation has been successfully grown by the flux method. The crystal perfection and its magnetic domain structure were investigated by X-ray double crystal topography of synchrotron radiation. The measured rocking curve of $^{57}\text{FeBO}_3(444)$ reflection without external magnetic field proved that the value of full width at half maximum (FWHM) was 4.48arcs for $\lambda=1.24\text{\AA}$. Precise topographs displayed, for the first time, the real image of a favorable magnetic multi-domain structure, which could support the high crystallinity of $^{57}\text{FeBO}_3$. As for influences of external magnetic field on $^{57}\text{FeBO}_3$ crystal perfection, the application of weak magnetic field (50Oe) hardly affected FWHM of rocking curve. However, the application of strong magnetic field (1300Oe) deformed the rocking curve profile drastically.

Keywords: FeBO_3 single crystal, rocking curve, X-ray topography, nuclear Bragg scattering, synchrotron radiation

1. INTRODUCTION

The antiferromagnet iron borate FeBO_3 single crystal is one of a few magnets combining transparency in the visible spectral range with spontaneous magnetization at room temperature. It is a weak ferromagnet with nearly antiparallel spin sublattices of Fe^{3+} ions in the (111) base plane at temperatures below the Néel point of 348.5K. The FeBO_3 crystal has a calcite structure belonging to the space group $R\bar{3}c(D_{3d}^6)$ ¹. In spite of many years and a large number of researches, there has been permanent interesting in studying the properties of FeBO_3 crystal. For examples, recent investigations have revealed a structural phase transition in FeBO_3 ², a collapse of the magnetic moment of Fe^{3+} iron under pressure³, and various dynamical phenomena, which include nonlinear effects⁴⁻⁶, magneto acoustic effects^{7,8}, photo-induced magnetic effects⁹. From the practical point of view, it has been pointed out that FeBO_3 single crystal can be applied to novel crystal monochromators of synchrotron radiation (SR)^{10,11}. Especially, ^{57}Fe -enriched $^{57}\text{FeBO}_3$ single crystal is the most advantageous optical element of nuclear resonant scattering of SR. Because, this optical element can emit a narrow band single-line radiation of 10^{-8}eV order by using the pure nuclear Bragg scattering (NBS) of $^{57}\text{FeBO}_3$ single crystal at the Néel temperature¹⁰. Then, it allows one to perform the energy domain Mössbauer measurement using excellent SR X-ray beam properties (linear polarization, small

beam size etc.) even in the multi bunch mode. However, as is described in ref 12 and 13, the natures of high refractivity and small divergence of NBS are achieved only when the nuclear monochromator crystal has a few arcsec order crystallinity. So that, available $^{57}\text{FeBO}_3$ single crystal is strongly required to have high crystal perfection. Besides, the influences of magnetic domain structures induced with external magnetic field on the crystallinity of $^{57}\text{FeBO}_3$ is important problem to develop the high performance Mössbauer single-line filtering element. Because, in order to control the polarization states of nuclear diffraction beam, the external field should be applied parallel to the crystal surface and perpendicular (or parallel) to the scattering plane to arrange the magnetic moment in one direction¹⁰.

The present paper describes the flux growth of a high quality $^{57}\text{FeBO}_3$ single crystal and double crystal X-ray topography experiments in order to elucidate the natures of crystal perfection and their relation to the magnetic domain structures.

2. $^{57}\text{FeBO}_3$ CRYSTAL GROWTH

Single crystals of $^{57}\text{FeBO}_3$ were grown by a $\text{PbO-PbF}_2\text{-B}_2\text{O}_3$ flux method¹⁴⁻¹⁷. As for raw materials, $\alpha\text{-}^{57}\text{Fe}_2\text{O}_3$ (^{57}Fe enrichment 95%), PbO (Spec Pure Grade 99.99%) supplied by Mitsui Mining & Mfg. Co. and PbF_2 (Spec Pure Grade 99.995%), B_2O_3 (Spec Pure Grade 99.99) by Johnson Matthey Co. The optimized

flux growth conditions (starting flux compositions and temperature procedure) were determined with several preliminary ^{57}Fe non-enrich growth experiments. As the results, the composition of starting materials for $^{57}\text{FeBO}_3$ crystal growth was: 5.30g α - $^{57}\text{Fe}_2\text{O}_3$, 27.11g PbO, 12.70g PbF_2 , and 47.39g B_2O_3 . They were packed in a 150cc platinum crucible. The crystal growth was performed in an electric furnace in air using the following program: heating from room temperature to 950°C at a rate of 50°C/hr, keeping a soak temperature of 950°C for 24hr. After a rapid cooling to 905°C in order to avoid the crystallization of α - Fe_2O_3 and Fe_3BO_6 , it is cooled at a rate of 0.1°C/hr to 800°C. Then, in this temperature range, FeBO_3 is a thermodynamically stable phase. At the end of the growth period, the furnace was cooled naturally below 800°C by cutting the power current. The crystals were carefully separated from the solidified flux by treatment in hot dilute nitric acid for several hours. Most flux grown single crystals were little pieces, but it could get a few large size crystals too. Fig. 1 shows the best crystal selected as a conspicuous centimeter-sized plate like crystal without macroscopic defects (scratches or cracks). It has been used for the following described X-ray diffraction experiments.



Fig. 1. Flux-grown $^{57}\text{FeBO}_3$ single crystal whose thickness is about 84 μm .

3. X-RAY DOUBLE CRYSTAL TOPOGRAPHY

3.1 Experimental setting

The experiments of X-ray double crystal topography with synchrotron radiation¹⁸⁾ were performed at BL-15C of Photon Factory (KEK). The experimental setting is represented in Fig. 2. In our studies, all measurements were performed on $^{57}\text{FeBO}_3(444)$ reflection in Bragg case geometry.

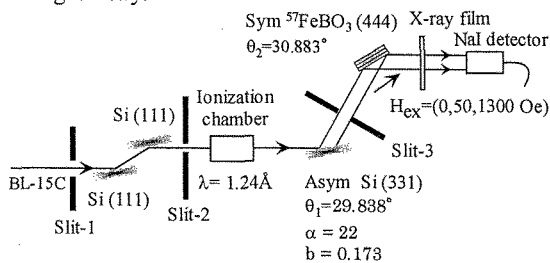


Fig. 2. Experimental setting of X-ray topography.

The synchrotron beam is tuned to $\lambda=1.24\text{\AA}$ by Si(111) double crystal monochromator and the intensity is monitored by an ionization chamber. X-ray is collimated by Si(331) with an asymmetry factor $1/b=5.78$. Then, the divergence of the delivered X-ray becomes very small ($\omega_h=0.75\text{arcs}$) in comparison with the diffraction width of $^{57}\text{FeBO}_3(444)$ reflection ($\omega_h=3.56\text{arcs}$). By using slit-3, X-ray beam is restricted with the size of 25mmx10mm, which is sufficient for illuminating the whole surface of the crystal. The optical arrangement of Si(331) and $^{57}\text{FeBO}_3(444)$ fulfills a condition of (+ -) parallel setting. The rocking curve profiles and X-ray topographs are obtained at three different conditions of

the external magnetic field: $H_{\text{ex}}=0, 50$ and 1300Oe. As is shown in Fig. 2, external fields are applied along the crystal surface to magnetize it parallel to the scattering plane. The topographs were recorded on nuclear plates Ilford L4 placed perpendicular to the diffracted beam.

3.2 Crystal perfection and magnetic domain structure

The crystal perfection was evaluated with the rocking curve of $^{57}\text{FeBO}_3(444)$ reflection in $H_{\text{ex}}=0\text{Oe}$. In such a case, antiferromagnet $^{57}\text{FeBO}_3$ single crystal has multi magnetic domain structure. The result is shown in Fig. 3.

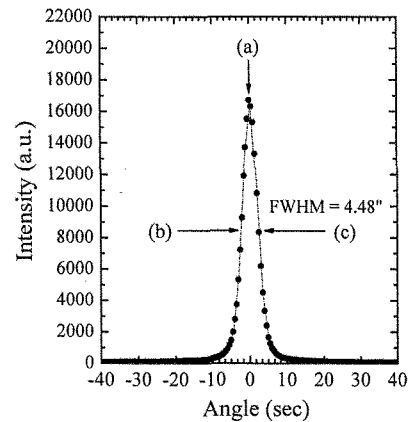


Fig. 3. Rocking curve with X-ray illuminating the whole sample in $H_{\text{ex}}=0\text{Oe}$. a) $\Delta\theta=0.0\text{arcs}$, b) $\Delta\theta=-2.24\text{arcs}$, c) $\Delta\theta=+2.24$ arcs. The dashed line is a gaussian fitting curve.

The profile of rocking curve shows a very sharp single peak form without any broad tails, and its FWHM is just only 4.48 arcsec. Since the theoretical FWHM of $^{57}\text{FeBO}_3(444)$ reflection at $\lambda=1.24\text{\AA}$ is 3.65 arcsec in this experimental setting, the measured FWHM coincides with the calculated value within 1.0 arcsec precisely. It implies that there are not any curvatures and growth boundaries in the crystal surface beyond a few arcsec. Therefore, it is concluded that this $^{57}\text{FeBO}_3$ crystal has the ideal crystal perfection suited for an optical element using nuclear Bragg scattering of SR.

The magnetic domain structure was observed by X-ray topographs recorded at three different angle positions of rocking curve; the peak position (a), low and high angle positions (b), (c) corresponding to the half maximum of rocking curve {See, Fig. 3(a),(b) and (c)}. Since rocking curve has a steep gradient at angle positions of half maximum, X-ray diffraction images show the high strain sensitivity for the latter two cases. The recorded topographs are shown in Fig.4 (a), (b) and (c) respectively.

In the topograph recorded at the peak position, X-ray diffraction contrast is obtained in a homogeneous illumination from almost whole of the crystal (See Fig.4 (a)). It indicates that the crystal surface is free from serious lattice defects such as dislocations and inclusions. However, in staring into the topography, it can be also observed that several faint straight-line contrasts cross over the crystal surface. The line contrasts are caused by the change of magnetostrictive deformation across the 90° magnetic domain walls. Here, 180° domain walls are invisible in topographs^{19,20)}. As is shown in Fig. 4(b)

and (c), the clear images of domain wall contrast and domain configuration have been observed by strain sensitive topographs. The domain contrasts separated with 90° domain walls have been composed of a lot of black-and-white diamond-shaped strain sectors, and they are regularly arranged with typical sector size of a few millimeters. In addition, since the black and white contrasts of each sector have been reversed in Fig. 4(b) and (c) respectively, it is found that adjacent domains have a slight inclination to the opposite direction each other and this structure spreads over the whole crystal surface with angular misorientation below a few arcsec. The schematic representation is shown in Fig. 5.

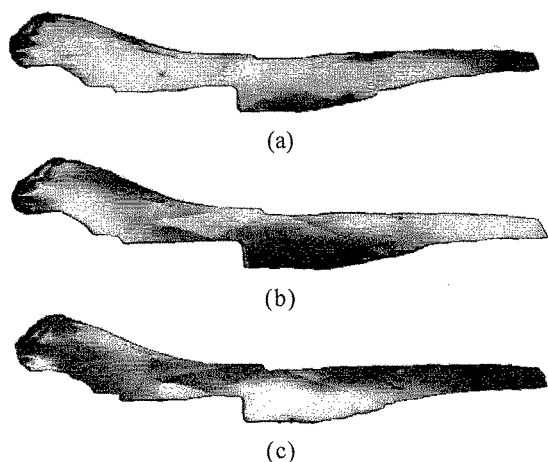


Fig. 4. X-ray double crystal topography of $^{57}\text{FeBO}_3$ (444) plane without external magnetic field. Topography (a), (b) and (c) are recorded at following angles; (a) $\Delta\theta=0.0\text{arcsec}$, (b) $\Delta\theta=-2.24\text{arcsec}$, (c) $\Delta\theta=+2.24\text{arcsec}$.

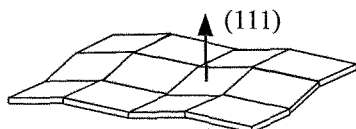


Fig. 5. Regularly arranged magnetic domain structure of a high quality $^{57}\text{FeBO}_3$ single crystal in $H_{\text{ex}}=0\text{Oe}$. It is divided into many diamond-shaped strain sectors by 90° multi magnetic domain walls.

These results are the first observation of a unique case that the regularly arranged multi magnetic domain structure realizes the high crystal perfection of $^{57}\text{FeBO}_3$. Usually, the multi magnetic domain structure of FeBO_3 single crystal is irregular and the direction of magnetization in domains distributes on the basal plane randomly. Consequently, the induced magnetostrictive strain gives rise to crystal imperfection^{17,21,22}.

3.3 Effect of magnetic field

The influences of external magnetic field on $^{57}\text{FeBO}_3$ crystal perfection were studied by rocking curve and topography of $^{57}\text{FeBO}_3$ (444) reflection placed in two different magnetic fields of 50Oe and 1300Oe. These values are enough large in comparison with saturation field of basal plane; $H_s \sim 5\text{Oe}$. So that, in both cases, the crystal has become single domain state magnetically. The measured rocking curves are shown in Fig. 6(a) and (b) respectively. The vertical axis has been normalized

by incident X-ray intensity of ionization chamber.

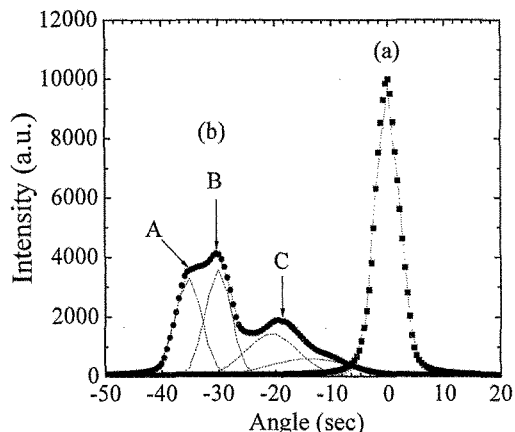


Fig. 6. Rocking curves of $^{57}\text{FeBO}_3(444)$ reflection placed in external magnetic fields; (a) $H_{\text{ex}}=50\text{Oe}$, (b) $H_{\text{ex}}=1300\text{Oe}$. The dashed lines are component curves of gaussian distribution fitting.

In Fig. 6(a), the rocking curve of weak magnetic field shows a single peak profile with a narrow FWHM of 4.85arcsec . It indicates that the transition of $^{57}\text{FeBO}_3$ crystal to single domain state hardly affects on the crystal perfection. In contrast, the application of strong magnetic field alters rocking curve profile dramatically. As is shown in Fig. 6(b), single peak of Fig. 6(a) splits into four low intensity peaks with the broad tails clearly (See component curves of gaussian fitting in Fig. 6(b)). From several repetitions of this measurement, it is found that the deformation of rocking curve is reversible process between $H_{\text{ex}}=50\text{Oe}$ and 1300Oe , and the switch on and off of strong magnetic field at angular position of Fig. 6(b), B makes realize the noiseless X-ray shutter on and off functions. On the other hand, topographs of $H_{\text{ex}}=1300\text{Oe}$ have been recorded at three different peak positions of rocking curve; Fig. 6(b) A, B and C. They are shown in Fig. 7(a), (b) and (c) respectively.

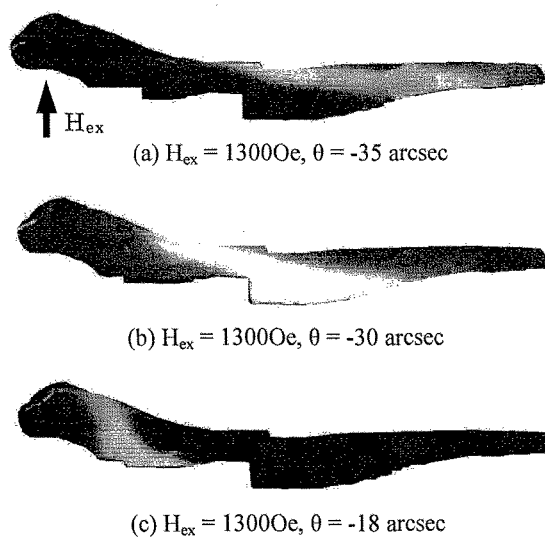


Fig. 7. X-ray double crystal topography of $^{57}\text{FeBO}_3$ (444) plane in $H_{\text{ex}}=1300\text{Oe}$. Topographs (a), (b) and (c) are recorded at different Bragg angles corresponding to angular positions of Fig. 6(b) A, B and C respectively.

In all topographs of Fig. 7, domain wall contrasts have been disappeared completely and X-ray diffraction contrasts are obtained in homogeneous illuminations from different parts of the crystal surface. The physical origins of these results are understood as follows. The application of magnetic field makes change $^{57}\text{FeBO}_3$ single crystal from multi magnetic domain structure to single magnetic domain structure. At the same time, the magnetic domain walls are vanished and it leads to the disappearance of domain wall contrast of topographs. So far as an external field is weak, crystal perfection is maintained yet. But, the application of strong magnetic field gives rise to the strong magnetostrictive strains in the crystal unevenly and it causes the local mechanical distortion on crystal surface. As the results, the observed white contrast of topographs changes the position from the right hand side to the left hand side with the increase of X-ray incident angle (See Fig. 7 (a), (b) and (c)).

4. CONCLUSIONS

In the present work, a very high quality ^{57}Fe -enriched $^{57}\text{FeBO}_3$ crystal suitable for Mössbauer single-line filtering element of SR has been successfully grown by the flux method. The crystal perfection and magnetic domain structure have been investigated by X-ray double crystal topography of SR. As the results, the following conclusions can be obtained about the influence of magnetic domain structure on the crystal perfection.

(a) In the multi-domain state, X-ray topographs have revealed that a unique strain structure is associated with regularly arranged multi-magnetic domains and it plays a vital role in the high crystal perfection of $^{57}\text{FeBO}_3$.

(b) In the single-domain state, it has been proved that the application of weak magnetic field ($H_{\text{ex}}=500\text{Oe}$) has hardly affected for the crystal perfection of $^{57}\text{FeBO}_3$.

(c) The application of strong magnetic field ($H_{\text{ex}}=1300\text{Oe}$) has induced the strong magnetostrictive strain in the crystal and it deformed the shape of rocking curve dramatically. This phenomenon makes it possible to control the intensity of X-ray diffraction by the magnitude of external field.

In the view point of futures application, X-ray double crystal topography of a high quality FeBO_3 crystal may be useful for the studies of magnetic domain properties in the nonequilibrium systems such as photo induced magnetization^{9,23} and magnetic super structure due to the ultra sound wave⁴. Since it allows us to observe the magnetic domain structure with high strain sensitivity of arcsec order.

ACKNOWLEDGMENTS

The authors are grateful to K.Hirano for kind guidance about BL-15C and PC control program of X-ray diffraction devices.

REFERENCES

- [1] R.Diehl, Solid State Commun.,**17**,743-5(1975).
- [2] A.G.Gavrilyuk, I.A.Troyan, R.Boehler, M.Eremets, A.Zerr, I.S.Lyubutin, V.A.Sarkisyan, JETP Letters.,**75**,25-7(2002).
- [3] I.A.Troyan, A.G.Gavrilyuk, V.A.Sarkisyan, I.S.Lyubutin, R.Rüffer, O.Leupold, A.Barla, B.Doyle, A.I.Chumakov, JETP Letters.,**74**,24-7(2001).

- [4] M.V.Chetkin, V.V.Lykov, JETP Lett.,**52**, 235-9 (1990).
- [5] L.E.Svistov, V.L.Safonov, L.Löw, H.Benner, J.Phys.: Condens.Matter., **6**, 8051-63 (1994).
- [6] Q.Z.Zhang, M.Mino, V.L.Safonov, H.Yamazaki, J.Phys.Soc.Jpn.,**69**, 41-4(2000).
- [7] I.Matsouli, V.V.Kvardakov, J.Baruchel, J.Appl.Cryst.,**33**,1051-8(2000).
- [8] T.Mitsui, Y.Imai, S.Kikuta, Nucl. Instr. and Meth. B., **199**,75-80 (2003).
- [9] I.V.Pleshakov, V.V.Matveev, J.Phys.: Condens.Matter.,**16**,1725-31(2004).
- [10] G.V.Smirnov, Hyperfine Interaction.,**125**,91-112(2000).
- [11] I.Matsouli, V.Kardakov, J.Espeso, L.Chabert, J.Baruchel, J.Phys.D: Appl.Phys.,**31**,1478-86(1998).
- [12] C.K.Suzuki, H.Ohno, H.Takei, F.Sakai, Y.Yoda, Y.Kudo, K.Izumi, T.Ishikawa, S.Kikuta, X.W.Zhang, T.Matsushita, M.Ando, Rev.Sci.Instrum.,**63**(1),1206-9(1992).
- [13] C.K.Suzuki, H.Takei, F.Sakai, Y.Yoda, X.W.Zhang, T.Mitsui, Y.Kudo, K.Izumi, T.Ishikawa, H.Sugiyama, M.Ando, H.Ohno, T.Harami, T.Matsushita, S.Kikuta, Jps.J.Appl.Phys.,**32**,3900-4(1993).
- [14] I.Bernal, C.W.Struck, J.G.White, Acta Cryst.,**16**,849-50(1963).
- [15] R.C.Lecraw, R.Wolfe, J.W.Nielsen, Appl.Phys.Letters.,**14**,352-4(1969).
- [16] H.Makram, L.Touron, J.Loriers, J.Crystal Growth.,**13/14**, 585-7(1972).
- [17] M.Kotrbova, S.Kadeckova, J.Novak, J.Bradler, G.V.Smirnov, Yu.V.Shvydko, J.Crystal Growth.,**71**, 607-14(1985).
- [18] T.Ishikawa, Rev.Sci.Instrum.,**60**, 2490-93(1989).
- [19] M.Polcarova, J.Kaczer, Phys.Status Solidi., **21**, 635-42(1967).
- [20] S.Nagakura, J.Chikaura, J.Phys.Soc.Jpn., **30**,495-515(1971).
- [21] G.B.Scott, J.Phys.D: Appl.phys.,**7**, 1574-87(1974).
- [22] V.G.Labushkin, A.A.Lomov, N.N.Faleev, V.A.Figin, Sov.Phys.Solid State., **22**(6), 1006 -10(1980).
- [23] M.Borovets, A.A.Garmonov, S.G.Rudov, Yu.M.Fedorov, JETP Lett., **50**,466-8(1989).

(Received December 23, 2004; Accepted January 31, 2005)